Journal of Physics: Conference Series **309** (2011) 012028 doi:10.1088/1742-6596/309/1/012028

Supernova Neutrino Detection in Water Cherenkov Detectors

Kate Scholberg

Department of Physics, Duke University, Durham, NC, 27708

E-mail: `schol@phy.duke.edu`

Abstract. This talk will describe sensitivity of past, current and future water Cherenkov detectors to a burst of supernova neutrinos.

1. Features of Water Cherenkov Detectors

Water Cherenkov detectors, in the form of large volumes of ultrapure water surrounded by photomultiplier tubes (PMTs), are sensitive to the charged particles produced by interactions of core collapse supernova neutrinos in the few to few tens of MeV range. Charged particles moving faster than the speed of light in a medium produce Cherenkov photons if $\beta > 1/n$, where n is the refractive index of the medium. Water is a convenient and cheap detector material, suitable for neutrino detection because very large volumes can be deployed cheaply, even though light yields are typically much lower than for scintillator. With index of refraction $n \sim 1.34$, the (total energy) Cherenkov threshold for electrons is 0.8 MeV; for muons the threshold is 160 MeV and for protons it is 1400 MeV. Energy loss is proportional to the number of photons detected, and one may reconstruct the charged particle's interaction vertex and direction via the Cherenkov ring pattern (which has angle of 42° for relativistic particles). However it is important to remember that heavy particles may be invisible in Cherenkov detectors, and signals from low energy electrons, positrons and gammas (which are detected via Compton-scattered electrons) may be lost.[1]

2. Past, Current and Future Water Cherenkov Detectors

Table 1 lists past, current and future supernova-neutrino-sensitive water Cherenkov detectors.

Famous past water Cherenkov detectors are the IMB and Kamiokande-II detectors, which both observed the burst from SN1987A, with 19 events collected between them [1, 2]. SNO, with 1.7 kton of light water and 1 kton of heavy water, ran from 1999 to 2006, although no supernova burst was observed during that time [3]. The only current example of a large water Cherenkov detector is Super-Kamiokande (Super-K), which has been running since 1996 [4]; Super-K's data-taking phases are shown in Tab. 1. Super-K is currently running with an energy threshold of about 4-5 MeV. A number of very large next-generation detectors are currently under

[1] Note that long string ice- or water-based detectors like IceCube and Antares also detect Cherenkov photons from supernova bursts. Although these detectors have very good timing capabilities, they do not reconstruct interactions event by event. IceCube's supernova capabilities were described in a separate presentation at this symposium; therefore long string water Cherenkov detectors will not be addressed here.

Table 1. Summary of past, current and future water Cherenkov detectors with supernova neutrino sensitivity.

Detector	Location	Fiducial Mass (kton)	PMTs (diameter, cm)	Effective coverage	pe/MeV	Live dates
IMB-1	US	3.3	2048 (12.5)	1%	0.25	1982-1985
IMB-2	US	3.3	2048 (20)	4.5%	1.1	1987-1990
Kamiokande I	Japan	0.88	1000/948 (50)	20%	3.4	1983-1985
Kamiokande II	Japan	1.04	1000/948 (50)	20%	3.4	1986-1990+
Super-K I	Japan	22.5	11146 (50)	39%	6	1996-2001
Super-K II	Japan	22.5	5182 (50)	19%	3	2002-2005
Super-K III+	Japan	22.5	11129 (50)	39%	6	2006-
SNO	Canada	1/1.7 (D_2O/H_2O)	9438 (20)	54%	9	1999-2006
LBNE WC	US	100-300	TBD	10-40%	2-6	202x?
MEMPHYS	Europe	440	TBD	30-40%	$\sim$4-6	202x?
Hyper-K	Japan	540	TBD	$\sim$20%	5-6	202x?

development: these include the Long Baseline Neutrino Experiment (LBNE) water Cherenkov detector in the US (100-300 kton) [5], Hyper-K in Japan (540 kton) [6] and MEMPHYS in Europe (450 kton) [7]. For these, photosensors tend to be a driving cost; improvements to light collection and quantum efficiency, currently a focus of worldwide effort, are of great interest.

3. Interactions in Water at Supernova Neutrino Energies

The total number of events expected scales as $1/R^2$, where R is the distance to the supernova (a distance of 10 kpc, which is a bit beyond the center of the Milky Way, is usually taken as a standard). A few hundred events per kton within a few tens of seconds are expected at this distance; at underground sites under consideration for next-generation detectors, one expects a clean signal out to Andromeda. See Fig. 1.

The cross-sections for relevant interactions in water are shown in Fig. 2. Some of these cross-sections– in particular, charged current inverse beta decay $\bar{\nu}_e + p \rightarrow e^+ + n$ (IBD) and elastic scattering (ES) of neutrinos on electrons $\nu_{e,x} + e^- \rightarrow \nu_{e,x} + e^-$, which proceeds via both neutral current (NC) and charged current (CC) channels, are known to few percent or better level. In contrast, other interactions on ^{16}O nuclei have relatively large uncertainties, and cross-sections have never been measured in the few tens-of-MeV energy range.

IBD is overwhelmingly dominant in the supernova neutrino energy regime: water Cherenkov detectors are primarily sensitive to the $\bar{\nu}_e$ component of the flux. The primary observable is the Cherenkov radiation of the IBD positron. In principle one may also exploit the delayed coincidence between the positron signal and a signal from capture of a neutron to tag the interaction. For neutron capture on free protons, the time interval for neutron thermalization and capture is about 200 μs, and a 2.2 MeV gamma is released from the capture. A gamma of such low energy is difficult to detect in a large water Cherenkov detector (and the gammas from positron annihilation are below Cherenkov threshold and hence their Compton scatters are invisible).

A potential enhancement to improve detectability of the neutrons for IBD tagging is addition of a Gd-containing solute to the water [8]. (Gd addition has been used successfully in scintillation detectors). Gd has a huge cross-section for neutron capture (49,000 barns for natural Gd, in contrast to a 0.3 barn neutron capture cross-section for free protons); after swallowing a neutron,

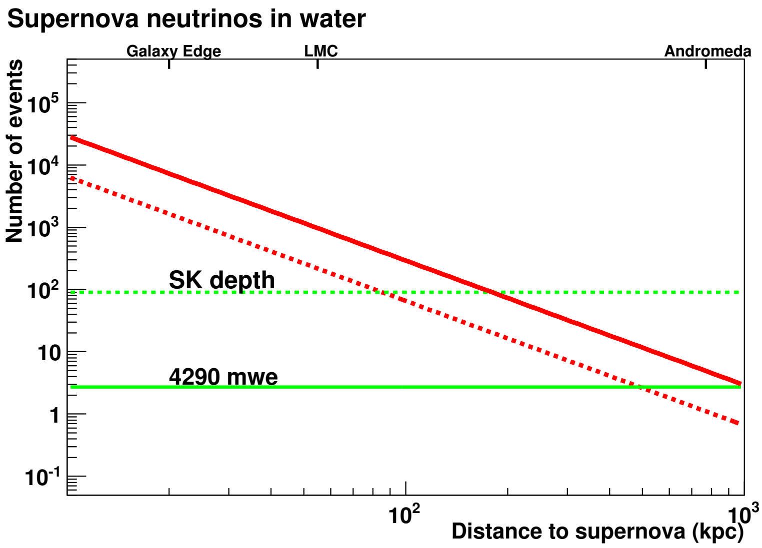

Figure 1. Approximate number of events detected as a function of distance to the supernova for Super-K (dashed line) and a 100 kton water detector (solid line). The horizontal green lines indicate cosmic muon rates at SK depth (∼2300 meters water equivalent (mwe)) and the Homestake mine depth (4290 mwe). (Note that cosmic muons can be effectively vetoed through several orders of magnitude.)

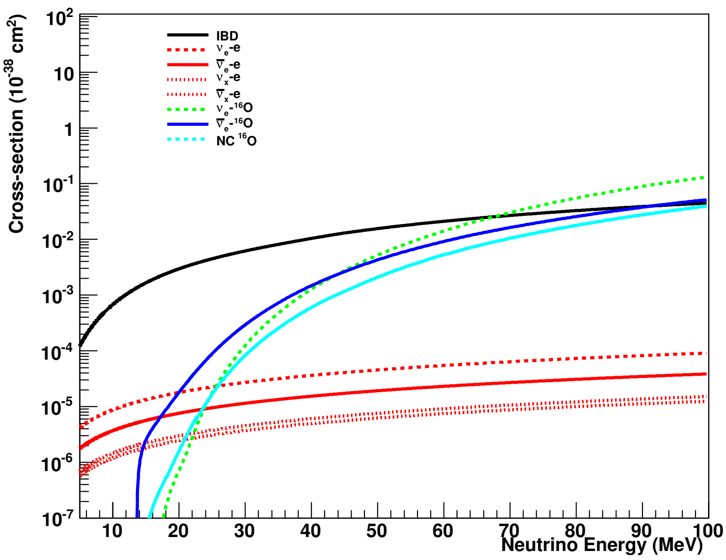

Figure 2. Cross-sections for relevant supernova neutrino interactions in water.

a Gd nucleus will release a cascade of gamma rays totalling about 8 MeV. Detection efficiency has been measured using a test setup in Super-K to be about 67% [9]. However note that because only about 4.5 MeV of energy per neutron capture is observed (because the gammas often Compton scatter electrons below Cherenkov threshold), good photocoverage is necessary to achieve this efficiency. Possibly improved analysis techniques, such as the use of isotropy information (as has been used for SNO in salt mode [10]), could be developed to improve neutron tagging efficiency. The Gd technique is under study for Super-K using a test tank [11], in order to answer questions of compatibility and purity of materials, feasibility of addition and removal of Gd, and neutron background.

Elastic scattering, although a relatively small component of the signal, is of significance because of its directionality. IBD positrons are emitted nearly isotropically, so are of little use for pointing. In contrast, electrons are kicked in the direction of the incoming neutrino, and the Cherenkov light cone allows determination of the charged particle direction. The pointing quality scales approximately as $\sim 25^\circ/\sqrt{N}$; degradation by isotropic background results in about 5 degrees pointing accuracy for a few hundred kton detector at 10 kpc [12, 13]. The pointing quality can be improved somewhat with the addition of Gd to reduce the isotropic background. The angular information can be also used to select a flavor-enhanced sample (see Section 5). Furthermore, if the direction to the supernova is known, neutrino energy can be more precisely reconstructed for ES events.

There are also non-negligible contributions from charged current interactions on oxygen, $\nu_e +^{16}\mathrm{O} \rightarrow e^- +^{16}\mathrm{F}$, $\bar{\nu}_e +^{16}\mathrm{O} \rightarrow e^+ +^{16}\mathrm{N}$, as well as neutral current excitations [14]. These reactions have diverse final states, including ejected nucleons and deexcitation gammas. These interactions are also asymmetric, and this asymmetry could potentially be of use in disentangling flavor components. However the cross-sections and final states for oxygen interactions in the supernova neutrino energy regime are relatively poorly understood both theoretically and experimentally.

4. Interaction Rate Calculation

I report here preliminary results from a study of event rates in a future large water Cherenkov detector, to be published in [15].

The predicted event rate from a supernova burst may be calculated by folding expected neutrino differential spectra with cross-sections for the relevant channels, and with detector response. We have performed the event rate computation by using estimated detector responses, making use of the GLoBES software [16]. We employ only the front-end rate engine part of GLoBES, and not the oscillation sensitivity part. GLoBES takes as input fluxes, cross-sections, "smearing matrices" and post-smearing efficiencies. The smearing matrices incorporate both interaction product spectra and detector response, determined using parameterized response functions or detector simulation output, or both. We are able to modify the smearing matrices to evaluate different detector configurations, such as for varied PMT coverages; in particular, we looked at 100 kton detectors with 30% and 15% coverages of high-quantum-efficiency PMTs (roughly corresponding to Super-K I and Super-K II capabilities). The software package used for the study will be made publicly available; the results should be generally applicable to any large water detector (as well as other detector types).

In this study, only the lepton in the final state for the CC interactions is considered, taking into account the energy threshold of the interaction. For the NC interaction with ^{16}O, $\nu_x +^{16}\mathrm{O} \rightarrow \nu_x +^{16}\mathrm{O}^*$, we are using a simplified model of the resulting deexcitation gammas by assuming relative final energy levels according to reference [14]. Because this reference does not provide differential final state information, we approximate the distribution of these levels to be independent of neutrino energy. The resulting gamma cascade was simulated using relative probabilities of the transitions for a given excited state; the resulting gamma spectrum was then run through the LBNE water Cherenkov detector simulation. We found rather poor efficiency for detecting these gammas, in contrast to the results in reference [17], due to the fact that gammas frequently scatter electrons below Compton threshold.

Figure 3 shows the resulting differential energy spectra for the different channels. The plot on the left shows the interaction rates as a function of neutrino energy. The plot on the right shows the distribution of observed event energies in the detector. Table 2 shows the breakdown of detected event channels, for two different specific supernova neutrino flux models, the "Livermore" [18] and "GKVM" models [19]. We note that different flux models can give substantially different event rates. In particular, because of the thresholds of the ^{16}O interactions, the rates of the CC interactions on oxygen are quite sensitive to the ν_e and $\bar{\nu}_e$ spectra.

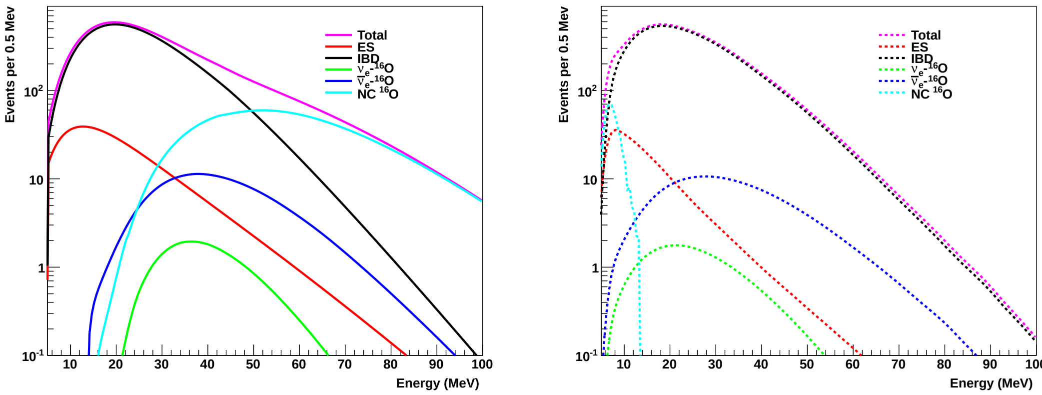

Figure 3. Event rates in water, for the Livermore model and a detector configuration with 30% high-quantum-efficiency PMT coverage (events per 0.5 MeV).

Channel	Events, "Livermore" model	Events, "GKVM" model
$\bar{\nu}_e + p \to e^+ + n$	27116	16211
$\nu_x + e^- \to \nu_x + e^-$	868	534
$\nu_e +^{16}\mathrm{O} \to e^- +^{16}\mathrm{F}$	88	379
$\bar{\nu}_e +^{16}\mathrm{O} \to e^+ +^{16}\mathrm{N}$	700	490
$\nu_x +^{16}\mathrm{O} \to \nu_x +^{16}\mathrm{O}^*$	513	124
Total	29285	17738

Table 2. Event rates for different models in 100 kton of water, for the 30% PMT coverage detector configuration.

Figure 4 shows the difference in observed event rates between the 15% and 30% PMT coverage configurations. For the 15% configuration, one loses about 10% of self-triggered events below $\sim$10 MeV. The loss includes most of the NC excitation events. (We note that clever triggering may mitigate this loss.)

5. Disentangling Flavors in Water

The addition of Gd to a water detector will not substantially change event rates, but will enhance ability to determine the flavor composition of an observed signal by allowing tagging of IBD events (although note that interactions on ^{16}O may produce ejected neutrons as well). To get some general idea of the value of neutron tagging of $\bar{\nu}_e$ we performed a simple study: we looked at flavor composition for tagged and untagged events. We assume that 67% of the true

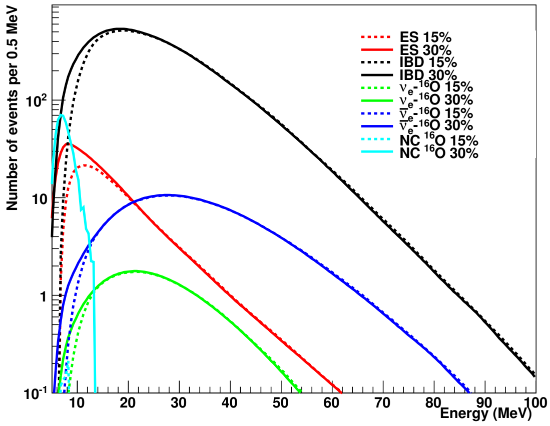

Figure 4. Comparison of event rates for 15% and 30% PMT coverage configurations in 100 kton of water.

IBD events will be tagged; we also assume that no events without a neutron will be falsely tagged as having a neutron (the false tagging rate should be $\sim 10^{-4}$ according to reference [9]). We also take into account CC and NC reactions of neutrinos on ^{16}O, for which some final states have neutrons; to estimate this contribution we use tables II, III and IV from reference [14]. Figure 5 shows the contributions of the different interaction channels for tagged and untagged events, for the GKVM flux. The neutron-tagged event rate is a nearly-pure IBD sample. The untagged event rate has contributions from elastic scattering (ES), and from CC and NC interactions on ^{16}O, but is dominated by untagged IBD.

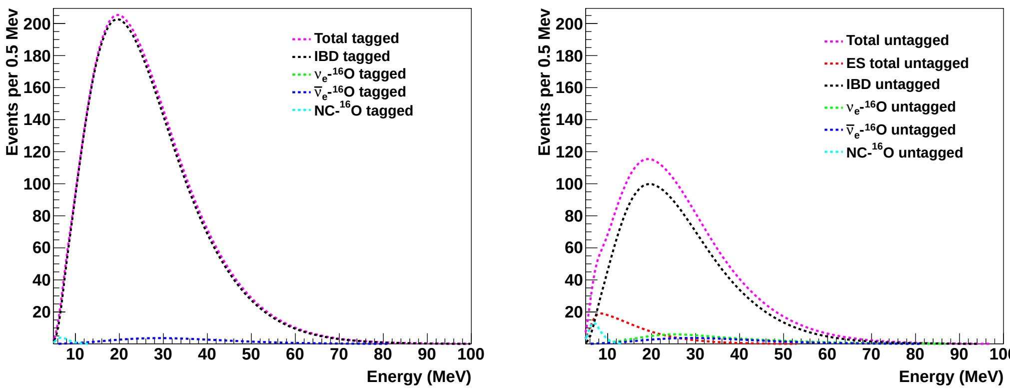

Figure 5. Total events in 100 kton of water showing contribution from the different interaction channels, for neutron-tagged (left) and untagged (right) events.

Figure 6 shows the contributions of the different neutrino flavors for tagged and untagged events. The tagged sample is nearly pure $\bar{\nu}_e$. The untagged sample has contributions from other flavors, and large contamination from untagged IBD $\bar{\nu}_e$.

Another potential method for selecting a flavor-enhanced sample in a water Cherenkov detector is to use the directionality of the neutrino-electron scattering signal: the ES sample is

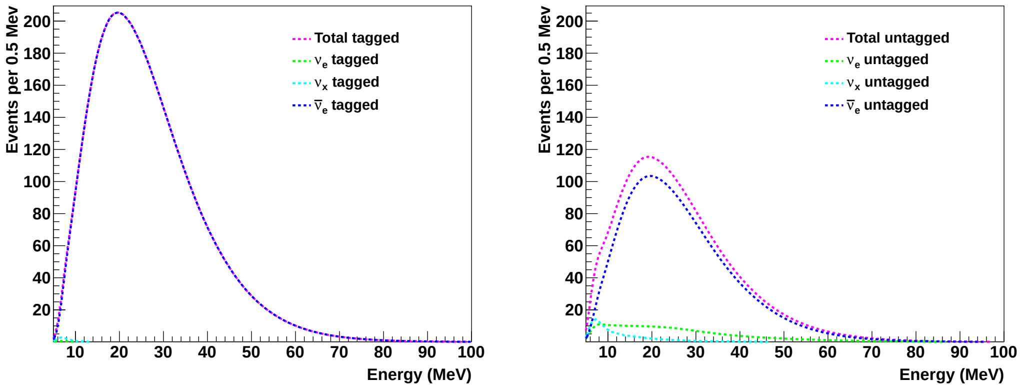

Figure 6. Total events in 100 kton of water showing contribution from the different flavors, for neutron-tagged (left) and untagged (right).

enriched in ν_e and ν_x relative to $\bar{\nu}_e$ We estimate the quality of a flavor-enriched ES sample by assuming that 66% of ES events will have $\cos\theta > 0.9$, where θ is the reconstructed angle of the scattered event [12]. Such a cut will reduce isotropic background by 95%. Figure 7 shows the interaction and flavor compositions of the "ES-enriched" sample selected by an angular cut, for the GKVM model. The non-ES background can be determined by counting events outside of the angular cut window.[2] Figure 8 shows the background-subtracted ES-enriched signal, with statistical error bars, for the GKVM flux. From Fig. 8 we can see that the ES component can be identified with high statistical significance. However the sample contains contributions from many flavors, and the relative amounts of the different contributions depend on the supernova flux.

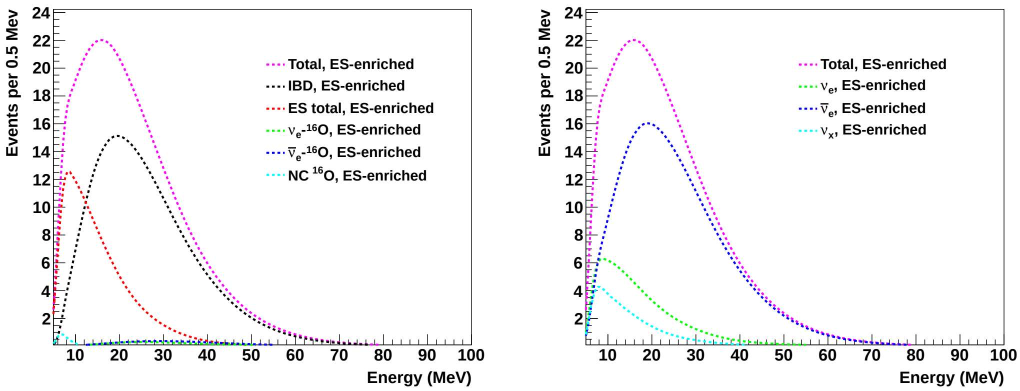

Figure 7. For the GKVM model, interaction (left) and flavor (right) composition of the ES-enriched sample in 100 kton of water.

One can also combine neutron-tagging and ES information, and imagine that there were an independent measurement of the ν_e flux from a liquid argon detector (or some other ν_e-sensitive

[2] We assume for the purpose of determining statistical uncertainty on the ES background subtraction that non-ES events have isotropic background, although that is not completely true– IBD events have a weak asymmetry, and interactions on ^{16}O have a backwards asymmetry.

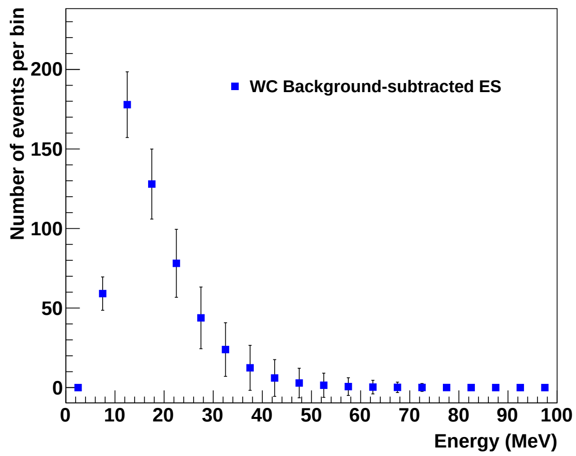

Figure 8. Background-subtracted ES signal in 100 kton of water in 5 MeV bins, for the GKVM flux. Error bars are statistical.

detector). In this case, one could in principle determine the ν_x flux, of considerable interest in itself. Figure 9 summarizes the total ES, $\nu_{e,xES}$, and ν_{xES} scattering rates for the GKVM flux, assuming both neutron-tagging and angular selection.

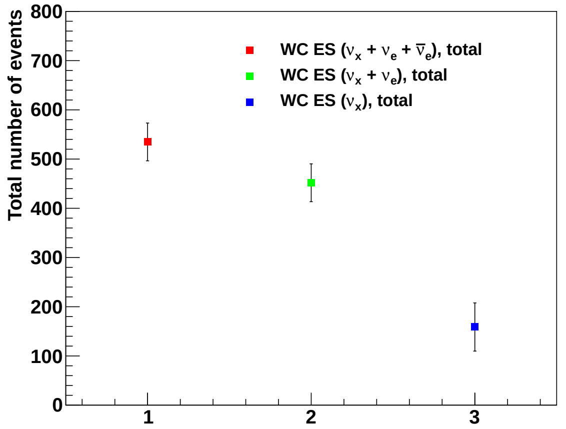

Figure 9. Inferred flavor components of a water Cherenkov ES signal, assuming neutron-tagging, angular selection, and a ν_e measurement from LAr, for the GKVM flux. Error bars include statistical and systematic contributions.

6. Summary

In summary, supernova neutrino detection with water Cherenkov detectors has a glorious past (IBM/Kamiokande-II detection of 1987A), a glorious present (Super-K) and, potentially, a glorious future: next-generation multi-hundred-kton scale detectors, possibly with neutron tagging using dissolved Gd, will provide an enormous signal for a nearby supernova. One expects a few hundred events/kton; most of these will be $\bar{\nu}_e$ from IBD, but other interactions contribute. ES is especially interesting because of its clean directionality. The supernova neutrino physics capabilities of a water Cherenkov detector will be enhanced by combination with other experiments' different flavor sensitivities.

Acknowledgments

The author wishes to thank the Long Baseline Neutrino Experiment Physics Working Group (and particularly the Supernova Burst Topical Group members Alex Beck, Farzan Beroz, Rachel Carr, Huaiyu Duan, Alex Friedland, Jim Kneller, Zander Moss, Diane Reitzner and David Webber) for contributions to this work.

References

[1] R. M. Bionta *et al.*, Phys. Rev. Lett. **58**, 1494 (1987).
[2] K. Hirata *et al.* [KAMIOKANDE-II Collaboration], Phys. Rev. Lett. **58**, 1490 (1987).
[3] C. J. Virtue [SNO Collaboration], Nucl. Phys. Proc. Suppl. **100**, 326-331 (2001). [astro-ph/0103324].
[4] M. Ikeda *et al.* [Super-Kamiokande Collaboration], Astrophys. J. **669**, 519-524 (2007). [arXiv:0706.2283 [astro-ph]].
[5] http://lbne.fnal.gov/index.shtml
[6] K. Nakamura, Int. J. Mod. Phys. **A18**, 4053-4063 (2003).
[7] A. de Bellefon, J. Bouchez, J. Busto *et al.*, [hep-ex/0607026].
[8] J. F. Beacom and M. R. Vagins, Phys. Rev. Lett. **93**, 171101 (2004) [arXiv:hep-ph/0309300].
[9] H. Watanabe *et al.* [Super-Kamiokande Collaboration], arXiv:0811.0735 [hep-ex].
[10] B. Aharmim *et al.* [SNO Collaboration], Phys. Rev. C **72**, 055502 (2005) [arXiv:nucl-ex/0502021].
[11] A. Kibayashi, f. t. S. -K. Collaboration, [arXiv:0909.5528 [astro-ph.IM]].
[12] J. F. Beacom and P. Vogel, Phys. Rev. D **60**, 033007 (1999) [arXiv:astro-ph/9811350].
[13] R. Tomas, D. Semikoz, G. G. Raffelt, M. Kachelriess and A. S. Dighe, Phys. Rev. D **68**, 093013 (2003) [arXiv:hep-ph/0307050].
[14] E. Kolbe, K. Langanke and P. Vogel, Phys. Rev. D **66**, 013007 (2002).
[15] LBNE Physics Working Group Study document, in preparation.
[16] http://www.mpi-hd.mpg.de/personalhomes/globes/
[17] K. Langanke, P. Vogel, E. Kolbe, Phys. Rev. Lett. **76**, 2629-2632 (1996). [nucl-th/9511032].
[18] T. Totani, K. Sato, H. E. Dalhed and J. R. Wilson, Astrophys. J. **496**, 216 (1998) [arXiv:astro-ph/9710203].
[19] J. Gava, J. Kneller, C. Volpe and G. C. McLaughlin, Phys. Rev. Lett. **103**, 071101 (2009) [arXiv:0902.0317 [hep-ph]].
[20] H. Duan and A. Friedland, arXiv:1006.2359 [hep-ph].